Bulletin of the Seismological Society of America, Vol. 94, No. 5, pp. 1728–1736, October 2004

Relationships between Instrumental Ground-Motion Parameters and Modified Mercalli Intensity in Eastern North America

by SanLinn I. Kaka and Gail M. Atkinson

Abstract A new relationship between modified Mercalli intensity (MMI) and peak ground velocity (PGV) is developed by comparing instrumentally recorded and inferred historical PGV values to observed MMI for 18 significant earthquakes from eastern North America (ENA), of moment magnitude 3.6–7.25. This PGV–MMI relationship is implemented in ShakeMaps in Ontario to estimate ground-shaking intensity (instrumentally derived MMI), given instrumental recordings of PGV. Corresponding relationships for 5% damped pseudoacceleration (PSA) at frequencies of 1, 5, and 10 Hz are also developed. We compare the results with previous relationships between MMI and ground motion parameters developed for California by Wald *et al.* (1999a) and Atkinson and Sonley (2000). We conclude that empirical relationships between MMI and ground motion are significantly different in eastern North America than in California. Thus, such relationships should be assessed for each region where ShakeMaps are implemented.

Introduction

ShakeMaps are computer-generated maps that indicate an earthquake occurrence, identify the area affected, and estimate the severity of ground shaking, providing a tool to rapidly assess and mitigate damage. The ShakeMap concept originated in California as part of the research and development efforts of the TriNet (California Institute of Technology, the California Division of Mines and Geology, and the U.S. Geological Survey). In California ShakeMaps, the intensity of ground shaking is inferred through an empirical relation between recorded peak ground acceleration (PGA), peak ground velocity (PGV), and modified Mercalli intensity (MMI) that was developed from observations in California (see Wald *et al.*, 1999b).

A comparable relationship between ground motion and felt intensity for eastern North America (ENA) is required in generating ShakeMaps that are applicable to ENA earthquakes. In contrast to California, events that generate strong shaking are rare in ENA. For ENA applications, then, we are interested in creating intensity ShakeMaps for the more frequent small-to-moderate events that may be widely felt but cause little to no damage (in addition to our interest in the larger events). Such maps are useful for public information purposes, particularly to nuclear utilities that must provide timely information on all felt events. Existing relations between MMI and PGV/PGA (e.g., Wald *et al.*, 1999a; Atkinson and Sonley, 2000) are not necessarily applicable to ENA because they were developed from California data. Earthquakes recorded in California have a lower frequency content than those recorded in ENA, and thus PGV and PGA have different meanings in the two regions. Moreover, the Wald *et al.* (1999a) relationship is not suitable for estimating intensity based on PGV at low-to-moderate intensity levels (see Wald *et al.*, 1999b), which are of interest in ENA applications.

PGV is the ideal choice among the ground-motion parameters for our ShakeMap applications, as it is the simplest and most rapidly available parameter from seismographic monitoring networks in ENA. It is also a parameter most directly related to kinetic energy, which in turns relates to damage. Wald *et al.* (1999a) showed that low levels of shaking intensity correlate fairly well with both peak ground acceleration (PGA) and PGV and high intensities correlate best with PGV. Boatwright *et al.* (2001) demonstrated that PGV is significantly better correlated with intensity than PGA, based on the correlation of the tagging intensity with observations of PGA and PGV in the 1994 Northridge earthquake.

We present empirical relationships between PGV and observed MMI by using data from 18 significant earthquakes from ENA, as listed in Table 1. Recorded ground-motion data are available for post-1982 earthquakes. We supplement these data with inferred PGV values from a few large historical events, as described in the next section. The same data are used to derive relationships between 5% damped pseudoacceleration (PSA) and MMI. These relationships are useful for engineering analyses keyed to a specific frequency.

Data Set for the Study

Most observed MMI data were obtained from the Geological Survey of Canada (GSC). For the 16 December 1811

Table 1
Study Earthquakes

No.	Date (mm/dd/yy)	**M**	Number of Recorded PGV Values	Number of Recorded PSA Values	Number of Estimated PGV Values (for **M** ≥5)	Number of Estimated PSA Values (for **M** ≥5)	Number of MMI Observations	Distance Range for Actual or Inferred Ground Motion (km)
1	12/16/1811	7.25			31	31	73	6–700
2	01/23/1812	7.0			16	16	49	6–700
3	03/01/1925	6.4			12	12	185	5–665
4	11/01/1935	6.2			28	28	1397	365–721
5	12/20/1940	5.1			55	55	350	25–265
6	09/05/1944	5.8			46	46	223	18–420
7	01/11/1982	5.2	17	11			747	138–724
8	01/19/1982	4.3	17	11			1154	209–537
9	10/07/1983	5.0	16	16			2519	145–832
10	11/25/1988	5.8	36	9			2569	51–708
11	10/19/1990	4.5	9	15			2215	170–468
12	11/16/1993	3.8	2	2			572	168–168
13	10/28/1997	4.2	3	3			40	318–388
14	11/06/1997	4.7	25	25			297	179–515
15	03/16/1999	4.6	6	6			26	98–405
16	01/01/2000	4.7	19	19			458	149–654
17	04/20/2002	5.0	62	62			2169	73–897
18	06/13/2003	3.6	20	20			23	23–100

and 23 January 1812 events (New Madrid earthquakes), MMI values were taken from work by Hough et al. (2000). MMI values for several historical earthquakes (1925, 1935, and 1940) are from the National Oceanic and Atmospheric Administration (NOAA) MMI database.

In general, MMI values are assigned based on a felt report, which is a description of the ground shaking experienced by the general public or an assessment of the damage level. For each instrumentally recorded event, we assigned an MMI value to every seismographic monitoring station based on general proximity to one or more MMI observations. Visual inspection of maps showing station locations and MMI assignments in the surrounding area was the preferred method of assigning MMI values. We assigned an MMI value to the station only whom we had reasonable confidence that the actual MMI value at the site would be within one unit of the assigned value (after Atkinson and Sonley, 2000). Some examples illustrate our approach. Figure 1a shows the MMI observations for the 2002 Au Sable Forks, New York, earthquake of **M** 5.0, together with the locations of seismographic monitoring stations that recorded the PGV and response spectra (PSA). For most recording stations, it is apparent that the MMI can be assigned within an uncertainty of 1 MMI unit. For example, the assigned MMI at HRV (Harvard) is 3, whereas at BINY it is 2. Figure 1b (MMI observations for the 1997 **M** 4.2 earthquake) illustrates the difficulty in assigning an MMI value with confidence in some cases. MMI 4 was assigned to station DAQ and the Charlevoix stations, but we could not assign MMI values to the remaining stations due to the lack of nearby MMI observations.

To obtain PGV and PSA values for events from 1993 and onward, we obtained horizontal- and vertical-component time series data from the GSC via their Automatic Data Request Manager facility (www.seismo.nrcan.gc.ca/nwfa/autodrm). We then processed the waveform data to remove instrument response and calculate PGV and PSA, using the strongest part of the record (see Atkinson, 2004). For events between 1982 and 1988, we used the existing database compiled by Atkinson and Mereu (1992). For the Saguenay earthquake of 25 November 1988, we obtained horizontal-component PGV values from strong-motion instruments (Munro and Weichert, 1989). Horizontal-component data were preferred when available. Where only vertical-component data were available, these were converted to equivalent horizontal-component values using the relationship of Atkinson (1993a) (see also Siddiqqi and Atkinson, 2001; Atkinson, 2004). Vertical-component data (converted to horizontal) comprise 43% of the PGV database. Because the stations are on hard rock (little site amplification), the horizontal and vertical-component motions are very similar and thus the horizontal-to-vertical (H/V) ratio is not a large factor (average $H/V = 1.2$).

For historical earthquakes, we estimated the horizontal-component PGV and PSA from the ground-motion relations for ENA, developed by Atkinson and Boore (1995), to allow expansion of our database to larger intensity. However, the Atkinson–Boore relationship applies to hard-rock sites, whereas the historical intensity data generally correspond to observations on soil. We account for this effect by applying a soil response factor, applicable to generically stiff-soil sites (NEHRP C), of 2.38 for PGV and 2.58, 1.94, and 1.39 for PSA at 1, 5, and 10 Hz, respectively, as suggested by Adams and Halchuk (2003). These factors are based on the difference in shear-wave velocity between stiff-soil and hard-rock sites, as discussed by Boore and Joyner (1997). We recog-

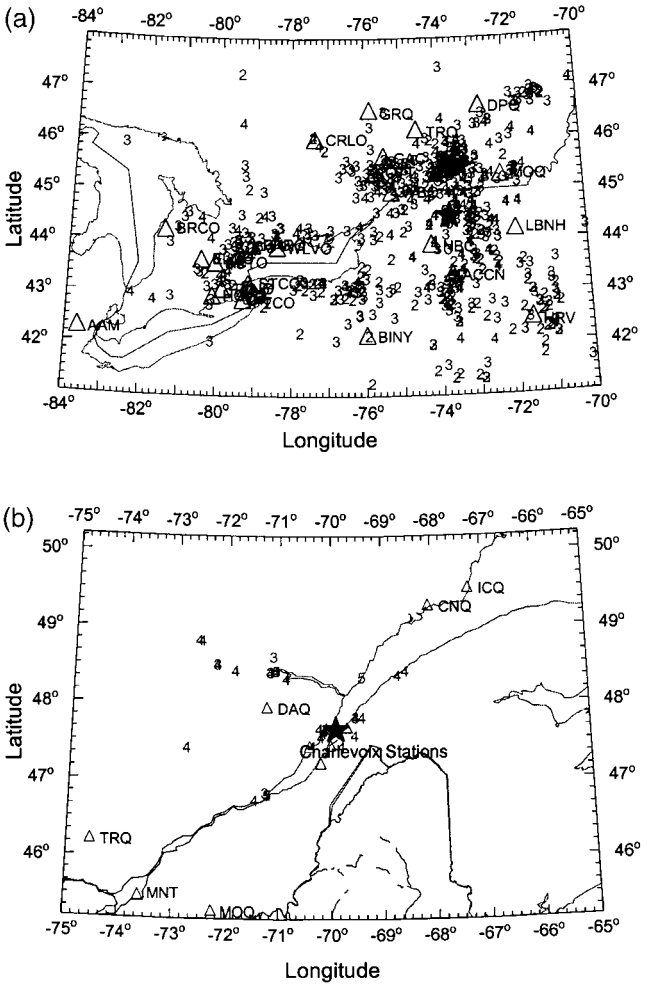

Figure 1. MMI observations and locations of seismographic monitoring stations that recorded the PGV and PSA values. Star shows epicenter. Numbers are MMI values. Triangles are stations. (a) 2002 **M** 5.0 earthquake (Au Sable Forks, N.Y.); (b) 1997 **M** 4.2 earthquake (Charlevoix, Que.).

nize that there is significant uncertainty in estimating ground motions of historical earthquakes by this process. Therefore, we checked these values carefully for consistency with those of the instrumentally recorded data. As we show in Figures 2 and 3, for intensity levels less than 5, typically corresponding to events with **M** <5, PGV values inferred using the Atkinson–Boore relation are significantly higher than recorded values. It is apparent that those estimated PGV values are not suitable for estimating the low intensities caused by small earthquakes. From Figure 3, we conclude that the Atkinson–Boore relations significantly overpredict PGV for events of **M** ≤5, which causes the observed discrepancies at low MMI levels. Thus, for historical earthquakes, we estimated PGV and PSA from the Atkinson–Boore relation using only those sites with MMI ≥5. At these intensity levels, the inferred values appear to be consistent with instrumental observations. However, we give these inferred values very little overall weight in view of these uncertainties.

In Figure 2, we also plot laboratory-based PGV ranges of some intensity levels, based on a study by McDaniel and Horton (2001). McDaniel and Horton performed shake-table tests to determine the velocity required to cause some of the typical phenomena associated with various intensities. They report that a velocity range of 0.1–0.3 mm/sec causes swaying of liquids (MMI I to II) and a range of about 10–100 mm/sec may be associated with spilling of liquids or stopping of a pendulum (MMI V). Results for ringing a bell (MMI VI) are more difficult to interpret but would also be consistent with a 10–100 mm/sec velocity.

Moment magnitude (**M**) values for the study events are from Atkinson and Chen (1997) for most of the historical events, Hough et al. (2000) for the New Madrid events, and Atkinson (2001) for most other events. For some small events, **M** values were estimated from the empirical relationship given by Atkinson (1993b).

PGV versus MMI Relations

Observed MMI and PGV for all the study events are displayed in Figure 2; we use different symbols to distinguish between actual recorded PGV and values inferred using the Atkinson–Boore relation for historical earthquakes. Because of the large scatter, the qualitative nature of observed MMI, and the uneven data distribution, a standard least-squares regression of MMI against PGV will not provide an unbiased prediction of MMI. To develop a robust relationship, we proceeded as follows:

1. We examined each MMI level independently and calculated the mean PGV corresponding to that particular MMI level (mean PGV values and corresponding standard deviations and number of observations are listed in Table 2). Inferred PGV values from the Atkinson–Boore relation are used only in calculating the mean for MMI ≥5.
2. We regressed MMI against the mean PGV, as shown in Figure 4, to obtain a simple relationship to predict MMI.

$$\text{MMI} = C_1 + C_2 \log \text{PGV}. \quad (1)$$

   Table 3 lists these C_1 and C_2 values along with their standard errors and the standard deviation of this prediction. MMI values of 9 and 10 were not used in the regression due to lack of data.
3. We evaluate magnitude and/or distance trends in the MMI residuals, calculated by subtracting predicted MMI (equation 1) from observed MMI. Figure 5 shows that there is a slight apparent trend to higher residuals at larger distances; this trend is more pronounced for PSA at high frequencies.
4. We regressed the MMI residuals versus distance to calculate correction factors to account for distance. Table 3 shows the coefficients for these regressions where C_3 and C_R are the coefficients of the regression of MMI residuals against distance:

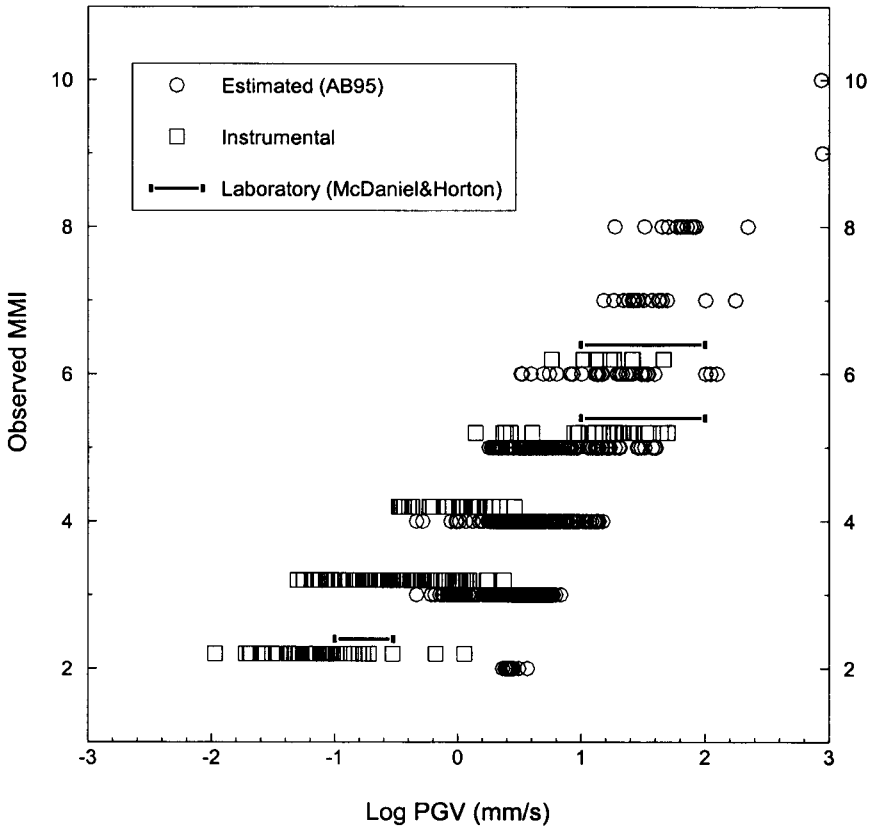

Figure 2. Observed MMI versus PGV for all data with squares representing recorded PGV and circles representing inferred values, using the Atkinson and Boore (1995) relations. PGV ranges based on laboratory measurements of McDaniel and Horton (2001) are also shown. Slight offsets from actual MMI values are used for clarity.

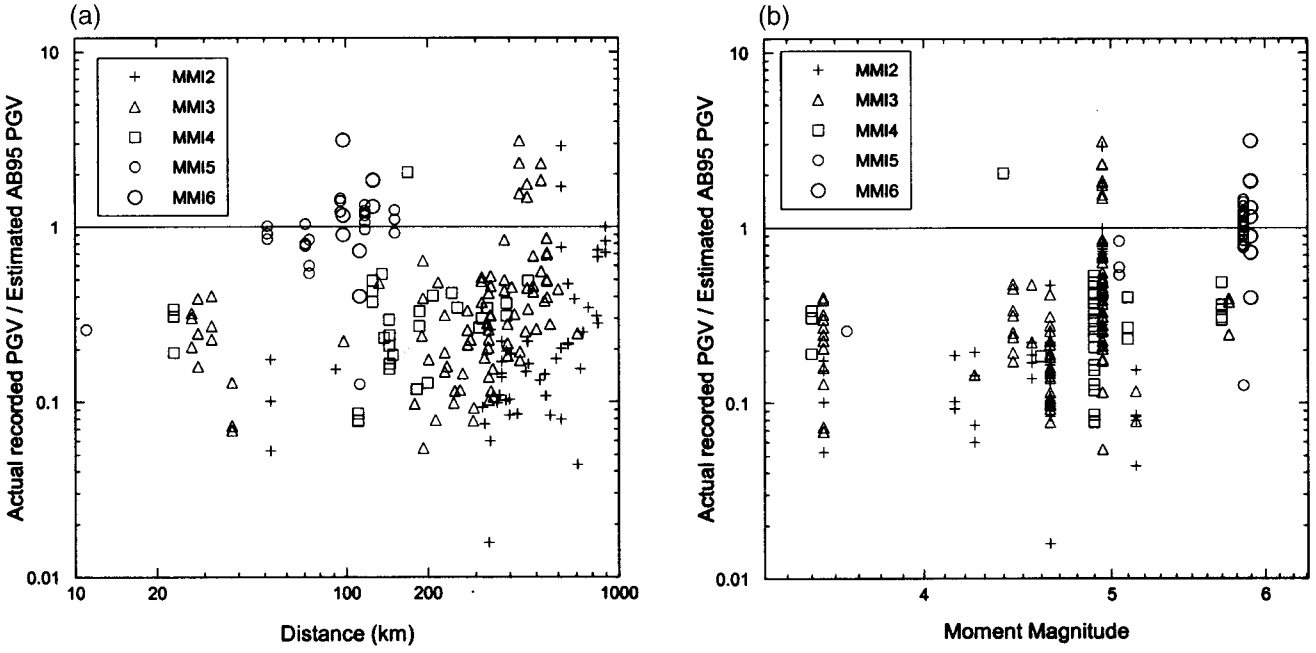

Figure 3. Ratio of actual recorded PGV to inferred PGV value using the Atkinson–Boore relation: (a) versus distance; (b) versus magnitude. Slight offsets from actual magnitude values are used for clarity.

Table 2
Mean PGV and PSA Values for Each MMI Level

MMI	Log PGV		Log PSA (1 Hz)		Log PSA (5 Hz)		Log PSA (10 Hz)		Number of Observations
	mm/sec	Std. Dev.	cm/sec/sec	Std. Dev.	cm/sec/sec	Std. Dev.	cm/sec/sec	Std. Dev.	
2	−1.1568	0.30	−1.2329	0.39	−0.3385	0.36	−0.4086	0.36	65
3	−0.4443	0.39	−0.6530	0.48	0.3206	0.41	0.2854	0.41	92
4	−0.0120	0.27	−0.1806	0.37	0.7663	0.25	0.9459	0.28	28
5	0.8366	0.31	0.7459	0.27	1.3178	0.32	1.1900	0.46	155
6	1.3642	0.19	1.3147	0.21	1.9620	0.15	1.9222	0.26	34
7	1.6692	0.19	1.5949	0.12	2.1711	0.18	2.1070	0.29	15
8	1.8549	0.23	1.8008	0.21	2.4095	0.26	2.3730	0.34	12

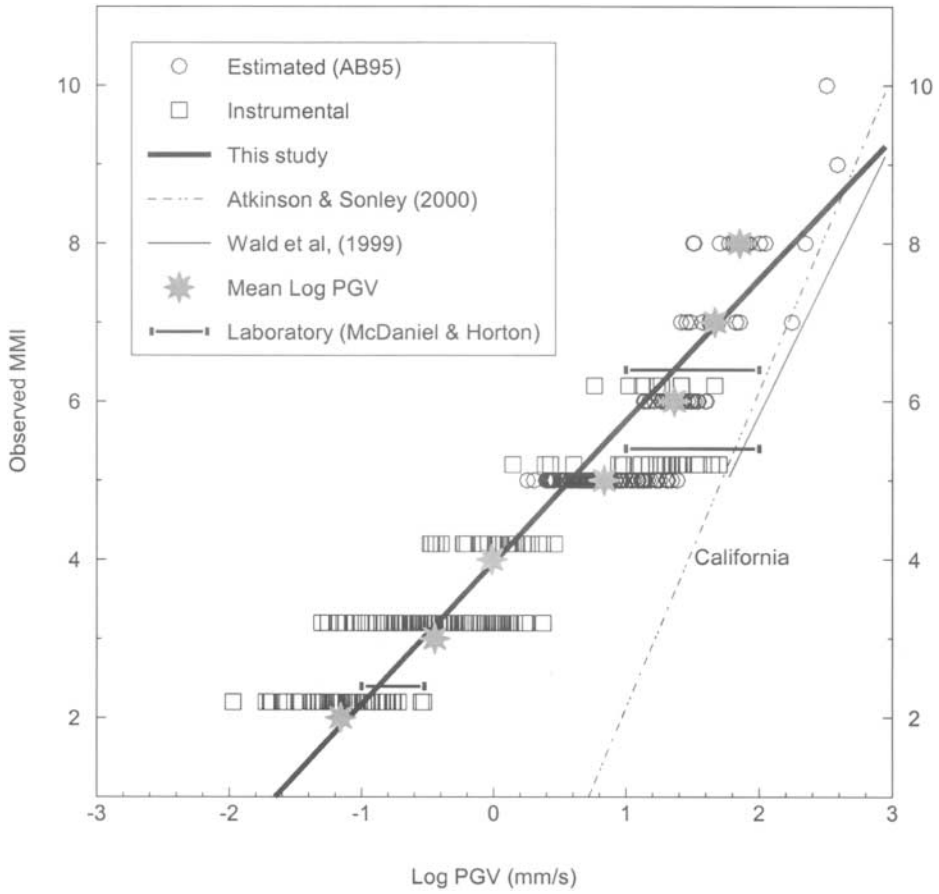

Figure 4. Observed MMI plotted against log PGV to obtain a simple MMI–PGV relationship (uncorrected for magnitude and distance dependencies). As a comparison, MMI–PGV relationships developed by Wald *et al.* (1999a) and Atkinson and Sonley (2000) are also shown in the figure. The Wald *et al.* (1999a) relation is truncated at MMI 5 because it is not applicable to lower intensity levels. PGV ranges based on laboratory measurements of McDaniel and Horton (2001) are also shown.

$$\text{MMI residual} = C_3 + C_R \log D. \quad (2)$$

We note that the trend with distance is significant for PGV and for PSA, especially at high frequencies.

5. We plotted distance-corrected residuals, obtained by subtracting off-distance trends in MMI residuals, as per equation (2), against magnitude. As shown in Figure 6, the corrected residuals are not significantly dependent on magnitude; thus, no magnitude term is necessary in our predictive relationship. We verified the lack of significance of magnitude trends by regression of corrected residuals versus magnitude.

6. We developed the final predictive equation:

Table 3
Coefficients of Equations and Their Standard Errors to Predict MMI from Instrumental Ground Motion Parameters

Y	PGV	PSA (1 Hz)	PSA (5 Hz)	PSA (10 Hz)
C_1	3.96	4.14	2.45	2.50
C_1 error	0.02	0.18	0.21	0.24
C_2	1.79	1.81	2.10	2.10
C_2 error	0.02	0.15	0.13	0.16
C_3	−0.12	0.88	−1.63	−3.10
C_3 error	0.17	0.18	0.18	0.19
C_R	0.28	−0.44	0.67	1.33
C_R error	0.07	0.07	0.07	0.08
σ_{1MMI}	0.72	0.83	0.76	0.90
σ_{3MMI}	0.65	0.68	0.68	0.68

(1) MMI = $C_1 + C_2 \log Y$, with standard deviation σ_{1MMI}
(3) MMI = $(C_1 - C_3) + C_2 \log Y - C_R \log D$, with standard deviation σ_{3MMI}

$$\text{MMI} = (C_1 - C_3) + C_2 \log Y - C_R \log D. \quad (3)$$

Table 3 provides the coefficients and their standard errors, along with the standard deviations of MMI values.

We repeated exactly the same procedure to obtain MMI–PSA relationships for PSA at 1, 5, and 10 Hz. The final predictive relations are given in Table 3.

Comparison to Other Relations

We compare this new relationship for ENA between PGV and MMI with those developed by Wald *et al.* (1999a) and Atkinson and Sonley (2000) from California data. To the best of our knowledge, there are no comparable studies completed for ENA or similar tectonic settings for testing and comparison to our result. However, the laboratory studies of McDaniel and Horton (2001) are relevant and lend support to our results.

In Figure 7, we plot our final MMI residuals (observed MMI − predicted MMI) for instrumental data in ENA (**M** 5.0–5.8) as a function of distance (less than 300 km), where the residuals are defined with respect to both ENA and western North America (WNA) predictive relations. The residuals show that our ENA relation provides a relatively unbiased estimate of observed intensity, whereas the WNA relations do not. These figures demonstrate that predictive relationships between MMI and ground-motion are significantly different in ENA than in WNA. Mean ground-motion values associated with any particular MMI value in ENA are significantly lower than those in WNA (see Tables 2 of this study and tables 2 and 3 of Atkinson and Sonley, 2000, for details). WNA predictive relations between MMI and ground motion significantly underpredict MMI for moderate ENA earthquakes.

The discrepancy between relations between MMI and PGV or PGA in ENA compared to those for California is not entirely surprising because of the different frequency content of motions in the two regions. We expect both PGA and PGV to be carried by higher frequencies in ENA than in California, and this may well impact their felt effects. However, the observed regional differences in relationships between MMI

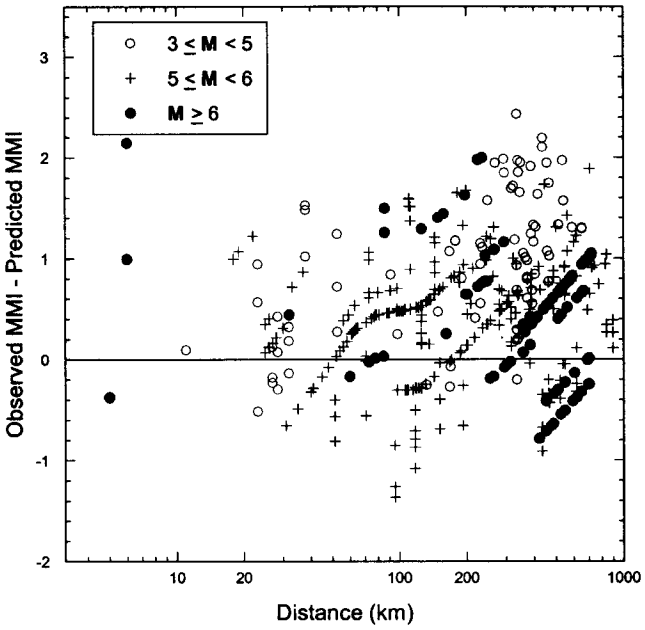

Figure 5. MMI residuals (observed MMI − predicted MMI from equation 1) plotted as a function of distance.

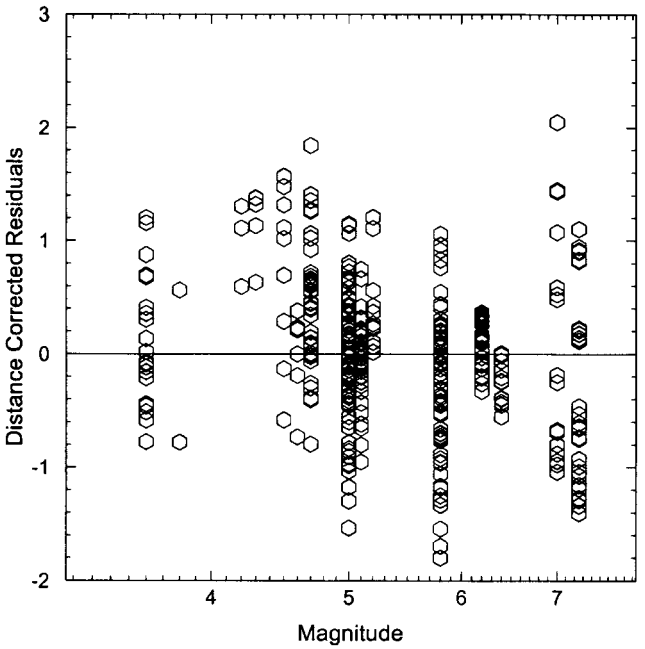

Figure 6. Distance-corrected MMI residuals (obtained by subtracting off-distance trends in MMI residuals, as described in the text) as a function of magnitude.

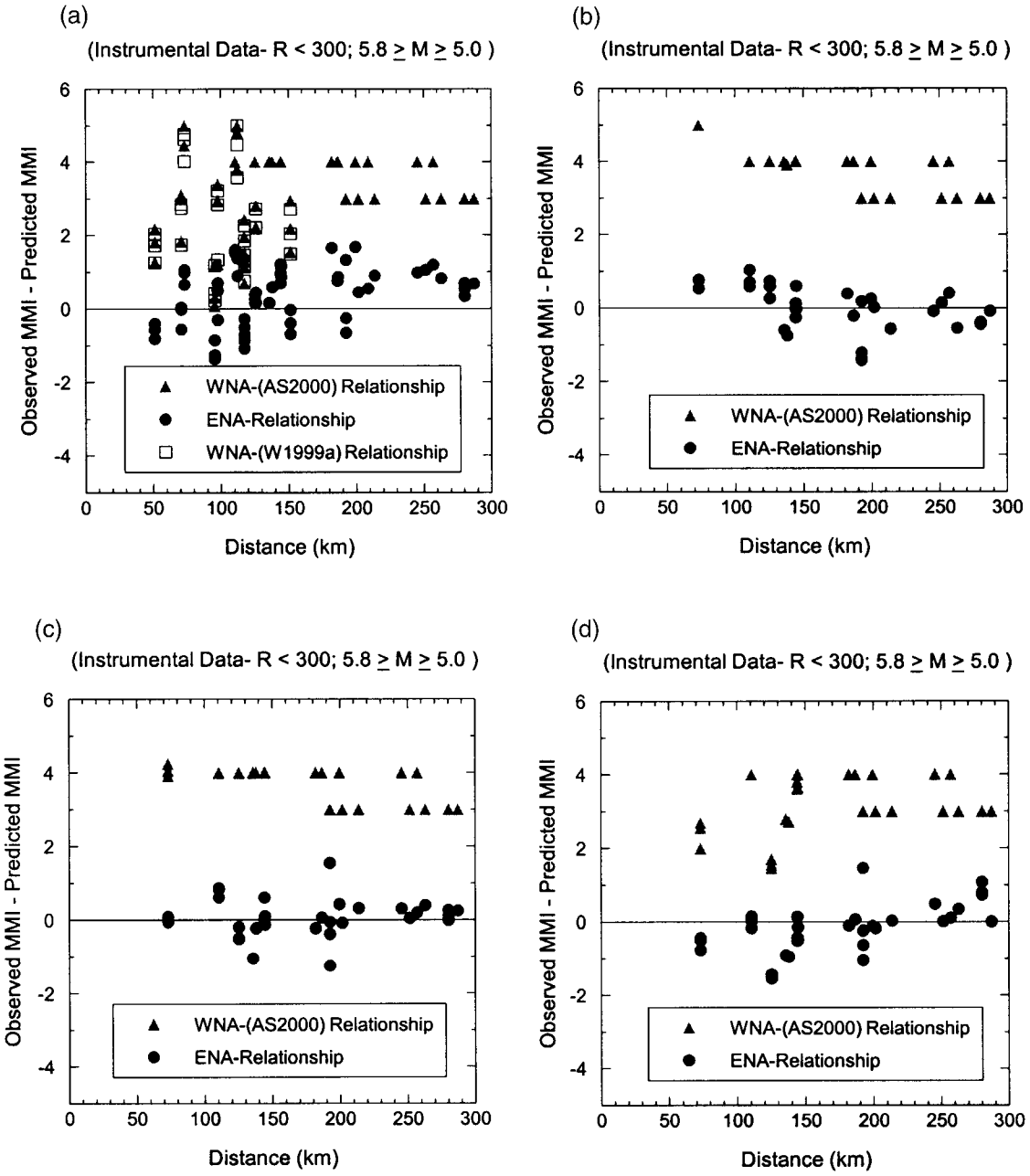

Figure 7. Comparison between MMI residuals for (a) PGV-based predictions; (b) PSA (1 Hz)-based predictions; (c) PSA (5 Hz)-based predictions; (d) PSA (10 Hz)-based predictions, using relations of this study (circles) and the California relations of Atkinson and Sonley (triangles) and Wald *et al.* (1999a) (squares). The Wald *et al.* (1999a) relation was not applied for MMI < 5.

and response spectra at a specific frequency are surprising and difficult to explain. Possible factors might be a longer duration of motion in ENA, allowing more time for the effects to be developed or noticed. Another factor might be frequency dependence of the effects associated with intensity observations. Alternatively, there may be regional discrepancies in the way MMI observations are compiled. Finally, it is possible that the recorded motions at seismographic sites are systematically low relative to motions experienced at nearby locations that reported the MMI value; this is a possibility because competent rock sites are sought for seismographic monitoring. At this time, these possibilities are presented only as speculations.

We examine the implications of our relations for ShakeMaps, using the 2002 Au Sable Forks, New York, **M** 5.0 earthquake as an illustration. Figure 8a shows the intensity map that is obtained using ground-motion relations for ENA (Atkinson and Boore, 1995) to predict PGA and PGV,

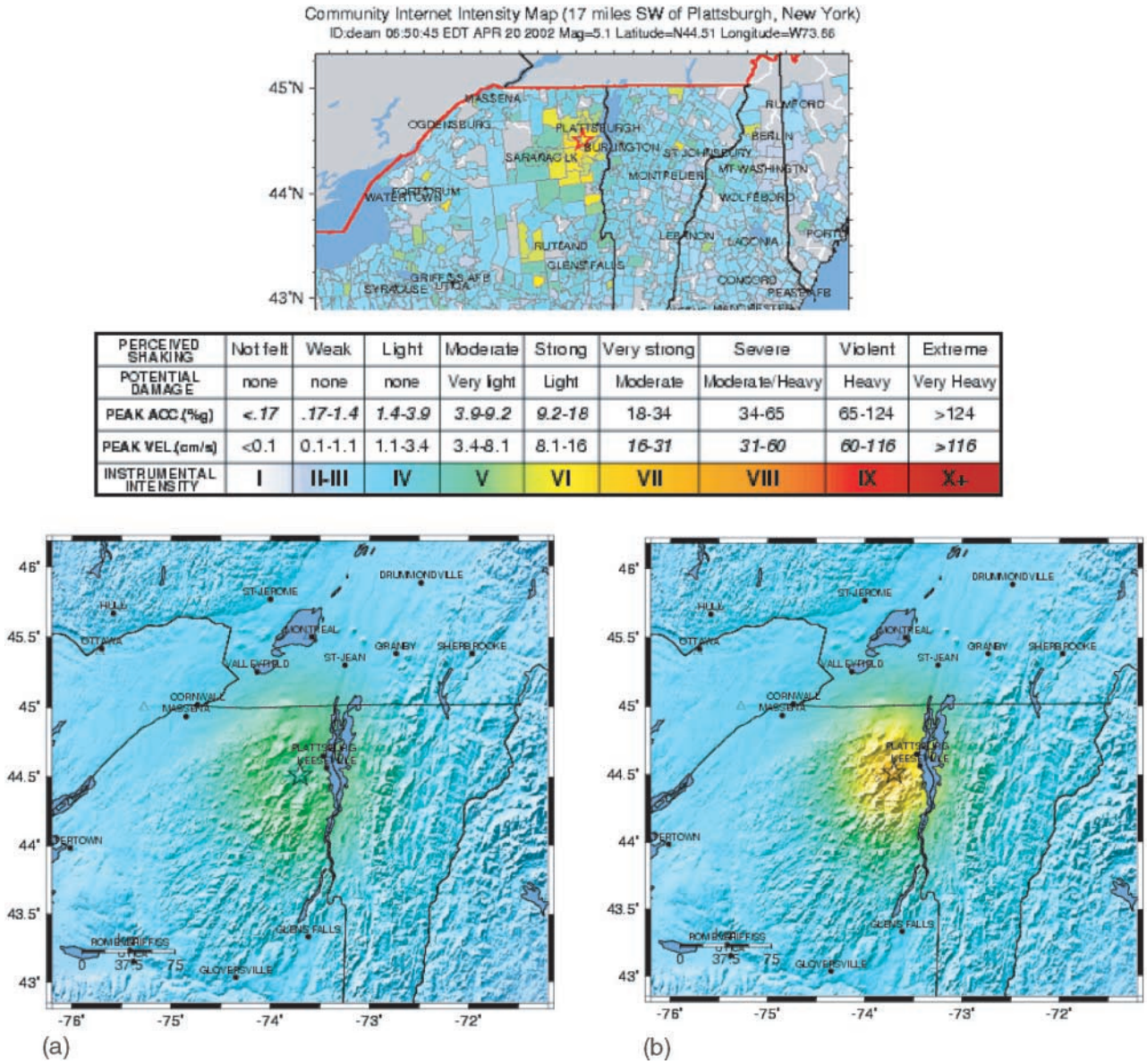

Figure 8. ShakeMap intensities for the 2002 Au Sable Forks, New York, **M** 5.0 earthquake. These maps use the Atkinson–Boore ENA ground-motion relations with (a) relations between PGV/PGA and intensity, developed by Wald *et al.* (1999a); (b) relation between PGV and intensity, developed in this study. Top panel shows observed intensities.

along with the instrumental intensity relations (PGA/PGV) for California, as prescribed by Wald *et al.* (1999a) and implemented in California ShakeMaps. (Note: An intensity map developed using ENA ground-motion relations (Atkinson and Boore, 1995) and the relationship between MMI and PGV/PGA developed from California data by Atkinson and Sonley (2000) is very similar to Fig. 8a). Figure 8b is the intensity map using ENA ground-motion relations (Atkinson and Boore, 1995) and the relationship between MMI and PGV developed in this study. The actual observed MMI map based on felt-reports submitted on-line (courtesy of U.S. Geological Survey) is shown in the top panel of Figure 8. We conclude from Figure 8 that when our new relationship between MMI and PGV is implemented in a ShakeMap, we obtain an MMI prediction that closely resembles the actual felt-reports. We note that local details are smoothed because of our lack of site-specific information on site response. By contrast, the ShakeMap developed with the Wald *et al.* (1999a) PGA/PGV versus MMI relations (or the Atkinson and Sonely [2000] relations) for California significantly underestimates the intensities from this event. Thus, predictive relations between MMI and ground motions are region specific, and these relationships should be carefully assessed for each region where ShakeMaps are to be implemented.

Conclusion

MMI values in ENA can be predicted, within about 1 MMI unit in most cases, from PGV or PSA, as shown in Table 3. PGV is the best predictive measure of MMI, based on the fact that it provides the lowest uncertainty in prediction (standard deviation of 0.65 MMI units). MMI can also be predicted from PSA; significantly higher MMI is predicted from a given PSA if the value was observed at distances close to the source. Uncertainty in predicting MMI from PSA is thus reduced if distance is included as a predictive variable (e.g., standard deviation of 0.76 versus 0.68 for PSA at 5 Hz).

For ShakeMap applications in southeastern Canada and the ENA, we recommend the use of PGV as the predictive variable for MMI, with the new relations developed in this study. Similar relations developed for California (e.g., Wald *et al.*, 1999a; Atkinson and Sonley, 2000) significantly underpredict MMI for ENA.

Data Sources

Instrumental Data

1. Canadian National Seismic Network (CNSN), Geological Survey of Canada (GSC), Automatic Data Request Manager facility (www.seismo.nrcan.gc.ca/nwfa/autodrm).
2. Ground Motion Database compiled by Atkinson and Mereu (1992) (available upon request).
3. Strong-motion records for the Saguenay earthquake of 25 November 1988 by Munro and Weichert (1989) (available at GSC, Open File 1996).

MMI Data

1. Geological Survey of Canada, Observatory Crescent (info@seismo.nrcan.gc.ca).
2. National Oceanic and Atmospheric Administration (NOAA), United States Department of Commerce (www.noaa.gov/).
3. Modified Mercalli intensity (MMI) data of the 1811–1812 New Madrid earthquakes given by Hough *et al.* (2000) (*J. Geophys. Res.* **105**, no. B10, 23,839–23,864).

Note: The database of MMI, PGV, and PSA observations compiled in this study is available upon request to skaka@ccs.carleton.ca.

Acknowledgments

We thank John Adams, Janet Drysdale, Nina Markova, and Stephen Halchuk from the Geological Survey of Canada for providing us with data. We thank Eleanor Sonley, Maurice Lamontagne, David Wald, and an anonymous reviewer for useful comments and suggestions.

References

Adams, J., and S. Halchuk (2003). Fourth generation seismic hazard maps of Canada: values for over 650 Canadian localities intended for the 2005 National Building Code of Canada. *Geological Survey of Canada Open File 4459*, 155 pp. Available from www.seismo.nrcan.gc.ca/hazards/recpubs_e.php

Atkinson, G. (1993a). Notes on ground motion parameters for eastern North America: duration and H/V ratio. *Bull. Seism. Soc. Am.* **83,** 587–596.

Atkinson, G. (1993b). Source spectra for earthquakes in eastern North America. *Bull. Seism. Soc. Am.* **83,** 1778–1798.

Atkinson, G. M. (2001). Linking historical intensity observations with ground-motion relations for eastern North America, *Seism. Res. Lett.* **72,** 560–574.

Atkinson, G. M. (2004). Empirical attenuation of ground motion spectral amplitudes in southeastern Canada and the northeastern United States, *Bull. Seism. Soc. Am.* **94,** 1079–1095.

Atkinson, G. M., and D. M. Boore (1995). Ground-motion relations for eastern North America, *Bull. Seism. Soc. Am.* **85,** 17–30.

Atkinson, G. M., and S. Z. Chen (1997). Regional seismograms from historical earthquakes in southeastern Canada, *Seism. Res. Lett.* **68,** 797–807.

Atkinson, G., and R. Mereu (1992). The shape of ground motion attenuation curves in southeastern Canada. *Bull. Seism. Soc. Am.* **82,** 2014–2031.

Atkinson, G. M., and E. Sonley (2000). Empirical relationships between modified Mercalli intensity and response spectra, *Bull. Seism. Soc. Am.* **90,** 537–544.

Boatwright, J., K. Thywissen, and L. Seekins (2001). Correlation of ground motion and intensity for the 17 January 1994 Northridge, California, earthquake, *Bull. Seism. Soc. Am.* **91,** 739–752.

Boore, D., and W. Joyner (1997). Site amplifications for generic rock sites, *Bull. Seism. Soc. Am.* **87,** 327–341.

Hough, S., J. Armbruster, L. Seeber, and J. Hough (2000). On the modified Mercalli intensities and magnitudes of the 1811–1812 New Madrid earthquakes, *J. Geophys. Res.* **105,** no. B10, 23,839–23,864.

McDaniel, R., and S. Horton (2001). Project SG-12: calibrating intensity with ground motions, Center for Earthquake Research and Information, *Student Leadership Council Online Magazine*, University of Illinois at Urbana-Champaign, http://mae.ce.uiuc.edu/Education/Student/Graduate/SCOJ/V2N2/RMcDaniel.pdf.

Munro, P. S., and D. Weichert (1989). The Saguenay earthquake of November 25, 1988 processed strong motion records, *Geol. Surv. Can. Open File 1996*, 150 pp.

Siddiqqi, J., and G. Atkinson (2001). Ground motion amplification at rock sites across Canada, as determined from the horizontal-to-vertical component ratio. *Bull. Seism. Soc. Am.* **91,** 877–884.

Wald, D. J., V. Quitoriano, T. H. Heaton, and H. Kanamori (1999a). Relationships between peak ground acceleration, peak ground velocity, and modified Mercalli intensity in California, *Earthquake Spectra* **15,** 557–564.

Wald, D. J., V. Quitoriano, T. H. Heaton, H. Kanamori, C. W. Scrivner, and C. B. Worden (1999b). 'Trinet ShakeMaps': rapid generation of instrumental ground motion and intensity maps for earthquakes in Southern California, *Earthquake Spectra* **15,** 537–556.

Department of Earth Sciences
Carleton University
Ottawa, Ontario K1S 5B6
Canada
skaka@ccs.carleton.ca
(S.I.K.)
gma@ccs.carleton.ca
(G.M.A.)

Manuscript received 24 October 2003.